Plasma ringing associated with pulsed resonance cones

P. M. Bellan

Plasma Physics Laboratory, Princeton University, Princeton, New Jersey 08540
(Received 21 June 1976; final manuscript received 8 December 1976)

A temporal wave packet of frequency $\omega_0(\omega_{ci}, \omega_{pi} < \omega_0 < \omega_{ce}, \omega_{pe})$ applied to a finite antenna in a magnetically confined plasma, is shown to excite an electrostatic field consisting of (1) a short-duration resonance cone and (2) a wave-like disturbance which follows afterward. This latter disturbance, which is related to the lower frequency mode of the delta-function induced transients discussed by Simonutti, persists long after the resonance cone. The phase factor associated with the disturbance is independent of ω_0, and its constant-phase surfaces are lines which emanate from the antenna and make a small angle θ with respect to the confining magnetic field **B**. θ decreases with increasing time so that "wavelengths" perpendicular to **B** also decrease with increasing time. The correspondence of the fields obtained by wave-packet excitation to those obtained by both cw and delta-function excitations is discussed and experimental results are reported.

I. INTRODUCTION

The cw behavior of resonance cones[1–4] differs from most other plasma waves. In particular, for resonance cones: the spatial profile is strongly localized (in fact, almost singular); the natural parameter is the angle of inclination relative to the confining magnetic field, rather than a wavelength; and the associated phase velocities are aligned at a right angle with respect to the group velocities. It is thus reasonable that the transient behavior of resonance cones should also be quite different.

Simonutti[5] has shown that a point source antenna driven by a short pulse (i.e., a temporal delta-function) excites a field having a broad frequency spectrum, and hence a spectrum of resonance cones both above and below the upper hybrid frequency each propagating along its characteristic angle. Felsen,[6] and Chen and Yen[7] have presented general theoretical analyses of transient wave phenomena in plasmas.

In this work we present theoretical and experimental studies of the field caused by imposing a temporal *wave packet* on a localized antenna. This wave-packet excitation is thus an intermediate case between the delta-function excitation of Ref. 5 and the cw excitation of Refs. 1–4, and in fact, by varying the wave-packet length it is possible to observe the transition to both of these limiting cases.

The main result of this work is that a temporal wave-packet excites a short-duration resonance cone which is followed by a wave-like disturbance, or wake. This wake remains long after the passage of the resonance cone and may be thought of as a spatial and temporal ringing of the plasma. The constant-phase surfaces of the wake are lines which emanate from the antenna and make a small angle θ with respect to the confining magnetic field **B**. θ decreases with increasing time so that wavelengths perpendicular to **B** also decrease with time. The existence of the wake was first observed experimentally; however for clarity, we shall first present the theory explaining why it occurs.

II. THEORY

A. Governing equations

For simplicity, we consider a homogeneous plasma confined by a uniform magnetic field $\mathbf{B} = B\hat{\mathbf{z}}$, and assume: (1) the wave is electrostatic, and (2) the driving frequency ω_0 is such that $\omega_{ci}, \omega_{pi} \ll \omega_0 \ll \omega_{ce}, \omega_{pe}$, so that ion and upper hybrid effects may be neglected. (Here, ω_{pe}, ω_{pi} are the respective electron and ion plasma frequencies; ω_{ce} and ω_{ci} are the respective electron and ion cyclotron frequencies.)

Let us now calculate the potential $\phi(\mathbf{x}, t)$ excited by a two-dimensional line source emitting a temporal wave packet. This source may be represented by a charge density ρ, where $\rho(\mathbf{x}, t) = \delta(x)\delta(z)\exp(i\omega_0 t - t^2/\tau^2)$. (Here, τ is the wave-packet duration time; the low frequency of the two modes discussed in Ref. 5 then corresponds to $\tau \to 0$.)

Using the standard cold-plasma two fluid equations, together with the assumptions (1) and (2), we find that

$$\phi(\mathbf{x}, t) = \int_{-\infty}^{\infty} d\omega \int_{-\infty}^{\infty} dk_z \int_{-\infty}^{\infty} dk_x \times \frac{4\pi\tilde{\rho}(\mathbf{k}, \omega)\exp(i\mathbf{k}\cdot\mathbf{x} + i\omega t)}{k_x^2 K_\perp + k_z^2 K_\parallel}, \quad (1)$$

where $\tilde{\rho}(\mathbf{k}, \omega) = \tau \exp[-(\omega - \omega_0)^2\tau^2/4]/(8\pi^{5/2})$, $K_\perp = 1 - \omega_{pi}^2/\omega^2 + \omega_{pe}^2/\omega_{ce}^2$, and $K_\parallel = 1 - (\omega_{pe}^2 + \omega_{pi}^2)/\omega^2$.

Proceeding to evaluate the integrals in Eq. (1), we complete the k_x integration path in the upper half-plane, and then use the method of residues. (The signs of the imaginary components of the poles are determined by, on the basis of causality, assuming that ω_0 has a small negative imaginary component. Then, noting that $\tilde{\rho}$ is peaked about ω_0, it is seen that the sign of k_z determines which denominator factor contributes a pole inside the k_x integration path.) After taking the derivative with respect to x to obtain the perpendicular field, E_x, the straightforward k_z integration is performed. Then, using the fact that $\tilde{\rho}$ is peaked about ω_0 to approximate $K_\perp \approx 1 + \omega_{pe}^2/\omega_{ce}^2$ and $K_\parallel \approx -\omega_{pe}^2/\omega^2$, we find

$$E_x \equiv \frac{-\partial\phi}{\partial x} = \sum_{\pm} \frac{\pm i\tau}{2\pi^{1/2}K_\perp} \int_{-\infty}^{\infty} d\omega \left(z \pm \frac{\omega_e^*}{\omega} x\right)^{-1} \times \exp[-(\omega-\omega_0)^2\tau^2/4 + i\omega t] , \quad (2)$$

where $\omega_e^* = \omega_{pe}/(1+\omega_{pe}^2/\omega_{ce}^2)^{1/2}$. By performing a time integration, and then changing to the dimensionless variables $\xi = (\omega - \omega_0)\tau/2$, $\beta = t/\tau$, and $a_\pm = (\omega_0 \pm \omega_e^* x/z)\tau/2$, Eq. (2) can be rewritten in a form more suitable for analysis, namely,

$$\int^t E_x \, dt' = \sum_{\pm} \pm I_\pm \exp(i\omega_0 t - t^2/\tau^2)/K_\perp , \quad (3)$$

where we have defined

$$I_\pm = \frac{\tau}{2\pi^{1/2}z} \int_{-\infty}^{\infty} d\xi \, \frac{\exp[-(\xi - i\beta)^2]}{\xi + a_\pm} . \quad (4)$$

Evaluation of Eq. (4) is now all that is required to find $\phi(\mathbf{x}, t)$.

B. Correspondence of the cw field

$\phi(\mathbf{x}, t)$ for the cw field ($\tau \to \infty$) is easy to calculate, since

$$\lim_{\tau\to\infty} I_\pm \approx \frac{\tau}{2z} Z(-a_\pm) , \quad (5)$$

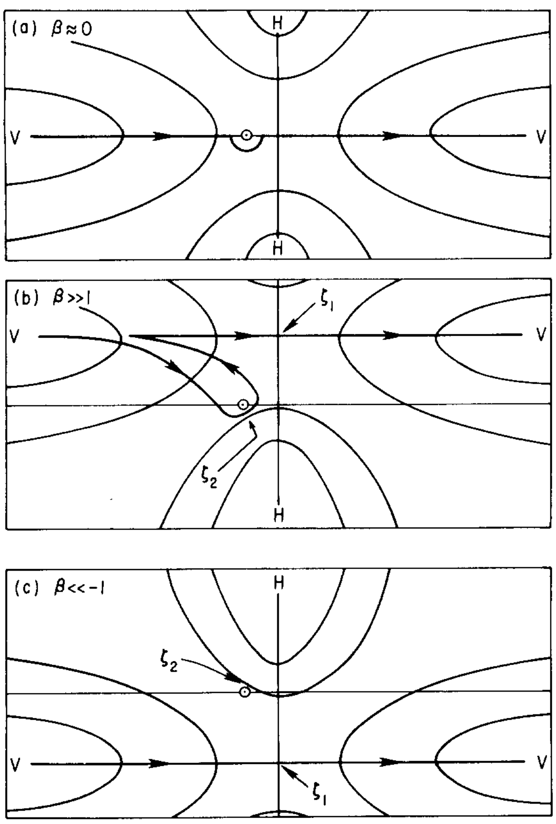

FIG. 1. Integration paths for Eq. (4). (a) Constant height contours for the Eq. (4) integrand when $\beta \approx 0$, heavy line is Landau integration path, H and V designate hills and valleys, ○ is the pole at $\xi = -a_\pm$; (b) corresponding contours for $\beta \gg 1$, integration path can be deformed to pass through the saddle points at both ξ_1 and ξ_2; (c) contours for $\beta \ll -1$, integration path can be deformed to pass through the saddle point at ξ_1 only.

where Z is the plasma dispersion function,[8] evaluated on the canonical Landau integration path. This path is shown in Fig. 1(a), together with the constant height contours of the integrand of Eq. (4). This particular path was chosen because it gives a solution corresponding to the well-known cw resonance cone [for example, cf., Eq. (26) of Ref. 4]. The correspondence may be observed by noting that the argument of Z is large (valid except exactly on the resonance cone) so that Eq. (5) can be rewritten as

$$\lim_{\tau\to\infty} I_\pm \approx \left[z\left(\omega_0 \pm \omega_e^* \frac{x}{z}\right)\right]^{-1} + i\pi^{1/2} \frac{\tau}{2z} \exp[-(\omega_0 \pm \omega_e^* x/z)^2\tau^2/4] . \quad (6)$$

Since in the limit $\alpha \to \infty$, $\alpha^{1/2}\exp(-\alpha x^2) \to \pi^{1/2}\delta(x)$ and also $\delta(ax) = \delta(x)/|a|$, we obtain

$$\lim_{\tau\to\infty} I_\pm \approx \frac{1}{\omega_0}\left[\frac{1}{z \pm (\omega_e^*/\omega_0)x} + i\pi \frac{|z|}{z} \delta\left(z \pm \frac{\omega_e^*}{\omega_0} x\right)\right] . \quad (7)$$

Using Eq. (7) to give $I_\pm$ in Eq. (3), and then taking the time derivative to obtain E_x, we see that the result indeed corresponds to the cw resonance cone.

C. Field during a short-duration resonance cone

Equations (6) and (3) also give the field behavior for short duration (i.e., finite τ) resonance cones, but only when the observation time is during the resonance cone (i.e., $|\beta| \ll 1$). Thus, during a pulsed resonance cone, the field looks like a cw resonance cone, except that the second term in Eq. (6) has a finite breadth determined by τ^{-1}.

D. Fields long after (before) a short-duration resonance cone

In contrast, the fields long after (or long before) a short-duration resonance cone are quite different from the cw field. Now $|\beta| \gg 1$, so that the contrast height contours of the integrand in Eq. (4) have either the form shown in Fig. 1(b) for $\beta \gg 1$, or Fig. 1(c) for $\beta \ll -1$. Standard steepest-descent integration techniques show that this integrand has saddle points at $\xi_1 = i\beta$ and at $\xi_2 = -a - i/(2\beta)$ [the locations of ξ_1 and ξ_2 are indicated in Figs. 1(b) and 1(c)]. As shown in Fig. 1(b), when $\beta \gg 1$ (i.e., long after a short-duration resonance cone has passed), the Landau path of Fig. 1(a) can be deformed to pass through both ξ_1 and ξ_2. Howevery, as shown in Fig. 1(c), when $\beta \ll -1$ (i.e., long before the resonance cone arrives), the Landau path can be deformed to pass through ξ_1 only.

Let us now calculate E_x for both $t \ll -\tau$ and $t \gg \tau$, keeping only terms of zero order in the small quantity $\exp(-t^2/\tau^2)$. After evaluating the saddle point integrals at ξ_1 and ξ_2, and then substituting for $I_\pm$ in Eq. (3) we obtain, for $t \gg \tau$ [Fig. 1(b)]

$$E_x \approx \sum_{\pm} (\tau\omega_e^* x/2^{1/2} z^2 K_\perp) \exp[-(\omega_0 \pm \omega_e^* x/z)^2 \tau^2/4 \mp i\omega_e^* tx/z] , \quad (8)$$

while for $t \ll -\tau$ [Fig. 1(c)]

$$E_x \approx 0 . \quad (9)$$

Equation (8) shows there exists a wave-like disturbance (or wake) which, since it is independent of $\exp(-t^2/\tau^2)$, persists long after the resonance cone has passed. Because the wake contains the amplitude factor $\exp[-(\omega_0 \pm \omega_e^* x/z)^2\tau^2/4]$, it is centered about the resonance cone trajectory, and also has a radial extent inversely proportional to τ. The phase factor, $\exp(\mp i\omega_e^* tx/z)$, is independent of the generator frequency ω_0, and most surprisingly, the x-direction wavelength associated with this phase becomes arbitrarily short with increasing time. We note that Eq. (8) is related to the second term of Eq. (7) in the following manner: For $\tau \to \infty$, the amplitude factor in Eq. (8) becomes a delta function, which then causes the phase factor to have the required $\exp(i\omega_0 t)$ time dependence.

By introducing the angle $\theta = \tan^{-1} x/z \approx x/z$, it is seen that the phase varies as $\exp(\mp i\omega_e^* t\theta)$ so that the surfaces of constant phases are lines, θ = const, passing through the antenna (this approximation breaks down as ω_0 approaches the upper hybrid frequency). For the situation described in Ref. 5 the amplitude factor is a constant because $\omega_0 = 0$ and $\tau \to 0$; thus, the lower frequency mode in Ref. 5 is determined solely by the phase factor. The temporal Fourier transform of the phase factor is a function of frequency and angle, and in agreement with Ref. 5, for a given frequency this function has its maximum amplitude at a θ corresponding to the angle of the cw resonance cone having the same frequency.

A physical interpretation of the weak phenomenon is that, because the exciting wave packet is a superposition of cw sinusoids each generating a cw resonance cone at a characteristic angle, the signal appearing at a given angle θ at late times (the wake) may be thought of as being caused by the particular sinusoidal component corresponding to θ.

III. EXPERIMENTAL MEASUREMENTS

The experiment was performed on the Princeton L3 machine ($n \approx 10^{10}$ cm^{-3}, $T_e \approx 2-5$ eV, $B \approx 1-2$ kG, plasma diameter approximately 10 cm, He gas, other parameters given in Ref. 9). Short ($\tau \approx 100$ nsec) rf bursts, an example of which is shown in Fig. 2(a), were applied to a single ring of the multiple ring structure described in Refs. 9 and 10. The resulting fields in the plasma were picked up by a radially traveling probe having two tips, radially separated by 1 mm. A subtracting transformer gave the difference signal (i.e., E_x) between the two tips; this signal was then amplified and fed into a Princeton Applied Research 162 boxcar integrator. Figure 2(b) shows the amplified E_x obtained when the probe was located inside the resonance cone, while Fig. 2(c) shows the marker for the 5 nsec wide boxcar gate. By plotting the boxcar output vs probe position for different gate delay times, it was possible to determine the dependence of the E_x profile on t/τ. Also by increasing the rf pulse length to approach the cw situation (i.e., $\tau \to \infty$), it was possible to observe the rela-

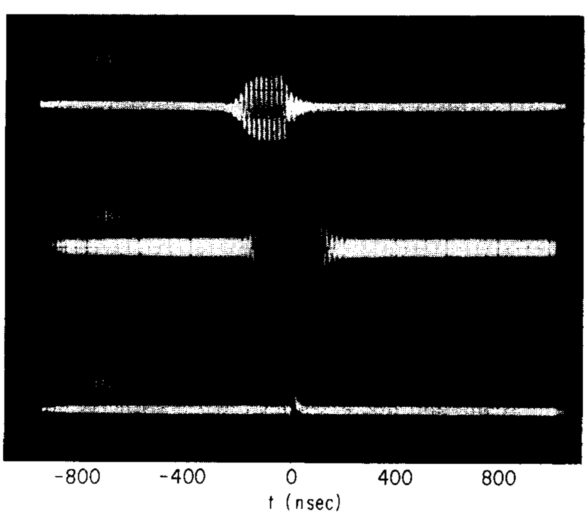

FIG. 2. Typical transmitted and received signals. (a) Waveform imposed on ring antenna, $\omega_0/2\pi = 50$ MHz; (b) corresponding signal received by the double-tip probe when located at the resonance cone peak; (c) boxcar gate position.

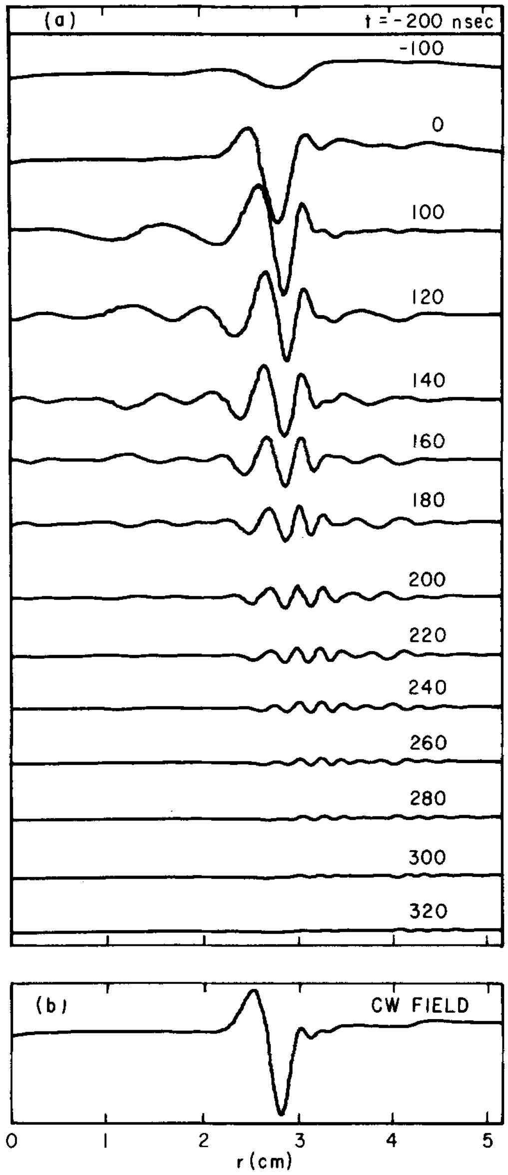

FIG. 3. E_x vs probe radial position. (a) E_x (boxcar signal) for sequence of gate delay times, times are relative to the origin of Fig. 2, and driving signal is that shown in Fig. 2(a); (b) cw resonance cone field.

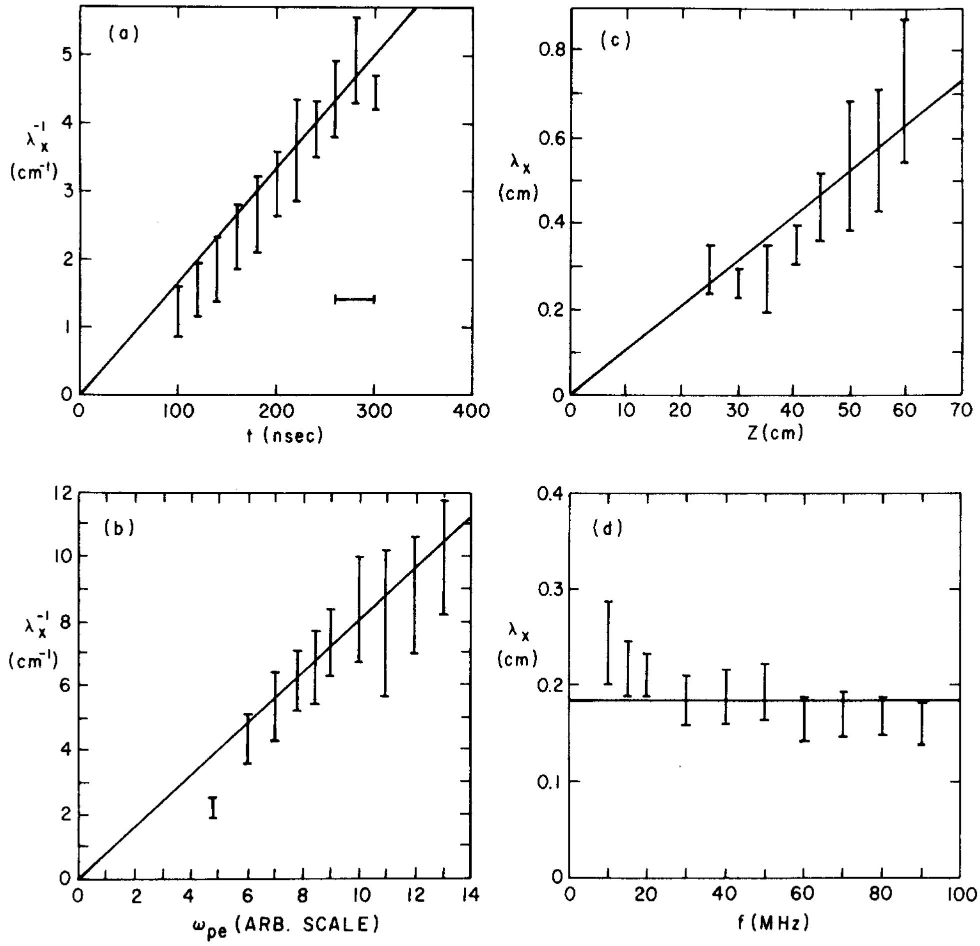

FIG. 4. Parametric study of wake phase. (a) λ_x^{-1} vs time, time origin as in Fig. 2; (b) λ_x^{-1} vs ω_{pe}, ω_{pe} variation obtained by changing the plasma equilibrium; (c) λ_x vs z obtained using rotating axial probe; (d) λ_x vs ω_0. In (a)–(d) solid lines indicate the behavior predicted by Eq. (8).

tion between the pulsed and cw fields.

Figure 3(a) shows examples of radial E_x profiles for a sequence of gate delay times. In agreement with Eqs. (9), (8), and (6), respectively, when $t \ll -\tau$, the field vanishes; when $|t|/\tau \ll 1$, the field is similar to the cw field [which is shown in Fig. 3(b)], and when $t \gg \tau$, the wake develops.

Figure 4 shows a parametric study of the phase factor of the wake. Since according to Eq. (8) this quantity varies as $\exp(\mp i\omega_e^* tx/z)$, the dependence of the observed x-direction wavelength, λ_x, on t, z, ω_{pe}, and ω_0 was measured. Figure 4(a) shows the inverse dependence of λ_x on t (time calibration as in Fig. 1). Figure 4(b) shows the dependence of λ_x on ω_{pe}, obtained by varying the filament current of the plasma source (ω_{pe}^2 was assumed proportional to the ion saturation current, the quantity actually measured; also for the parameters of the experiment, $\omega_{pe} \ll \omega_{ce}$, so that $\omega_e^* \approx \omega_{pe}$). By using the rotating axial probe described in Ref. 9, the linear dependence of λ_x on z was verified; this is shown in Fig. 4(c). Finally, Fig. 4(d) shows the independence of λ_x relative to ω_0. However, as expected, when ω_0 was varied, the radial location of the wake shifted, in the same way as a cw resonance cone would for a change in driving frequency. (The increase in λ_x for $\omega_0/2\pi < 20$ MHz occurs because at these lower frequencies the radial location shifts outward to be in a region of reduced density.)

To confirm the relation of the transient field to the cw field, the rf pulse length was increased to several hundred nanoseconds. It was then found that the cw field was obtained when the boxcar gate was inside the long pulse, but the wake field was obtained when the gate was located after the turn-off of the long pulse. The rf pulse length was also varied to check for the $\exp[-(\omega_0 \pm \omega_e^* x/z)^2\tau^2/4]$ dependence of the wake. Qualitative agreement was observed, in that the wake had a larger radial extent for very short pulses, but quantitative measurements could not be made due to difficulties in maintaining a Gaussian profile for arbitrary pulse lengths.

IV. SUMMARY

During a pulsed resonance cone the field is similar to that of a cw resonance cone. However, after the pulsed resonance cone has passed there exists a long lasting wave-like disturbance or wake. The constant-phase surfaces of the wake are lines which emanate from the antenna and make a small angle with respect to the confining field **B**. This angle decreases with increasing time so that the wavelengths perpendicular to **B** also decrease with increasing time. The wake phase is independent of the driving frequency and the components of its temporal Fourier transform behave like resonance cones. For very short wave-packets the wake field corresponds to the fields described by

Simonutti,[5] while for long wave-packets the field becomes the cw field. Experimental measurements are in good agreement with this description.

ACKNOWLEDGMENTS

The author wishes to thank Dr. K. L. Wong for his help in making some of the experimental measurements. The technical assistance of J. Johnson and J. Taylor is gratefully acknowledged.

This work was supported by the United States Energy Research and Development Administration Contract No. E(11-1)-3073.

[1] H. H. Kuehl, Phys. Fluids **5**, 1095 (1962).
[2] R. K. Fisher and R. W. Gould, Phys. Fluids **14**, 857 (1971).
[3] R. J. Briggs and R. R. Parker, Phys. Rev. Lett. **29**, 852 (1972).
[4] P. M. Bellan and M. Porkolab, Phys. Fluids **17**, 1592 (1974).
[5] M. D. Simonutti, Phys. Fluids **19**, 608 (1976).
[6] L. B. Felsen, IEEE Trans. Antenna Propag. **AP-17**, 191 (1969).
[7] K. C. Chen and J. L. Yen, Radio Sci. **8**, 51 (1973).
[8] B. D. Fried and S. D. Conte, *The Plasma Dispersion Function* (Academic, New York, 1961).
[9] P. M. Bellan and M. Porkolab, Phys. Fluids **19**, 995 (1976).
[10] P. M. Bellan and M. Porkolab, Phys. Rev. Lett. **34**, 124 (1975).